Data-driven dynamics simulation for railway vehicles

Yinyu Nie [a,b], Zhao Tang [a,*], Fengjia Liu [a], Jian Chang [b], Jianjun Zhang [a,b]

[a] *State Key Laboratory of Traction Power, Southwest Jiaotong University, Chengdu, 610031, P.R. China*

[b] *National Centre for Computer Animation, Bournemouth University, Poole BH12 5BB, U.K.*

* Corresponding author at: State Key Laboratory of Traction Power, Southwest Jiaotong University, Chengdu 610031, Sichuan, China.

Email address: tangzhao@swjtu.edu.cn (Zhao Tang)

Data-driven dynamics simulation for railway vehicles

Abstract: Sophisticated finite element (FE) model are usually critical for the research and simulation of vehicle dynamics, especially for train crash cases. However, factors such as the complexity of the meshes, the distortion problems involved in a large deformation, etc. would undermine the calculation efficiency of a FE model. Its alternative, a multi-body (MB) model, shows a satisfying time efficiency though, it only presents a limited simulation accuracy when involving highly nonlinear characteristics in a dynamic process. To maintain the advantages of both the two methods, this paper proposes a data-driven simulation framework to model the dynamic behaviours of railway vehicles. In this framework, by extracting the training data of FE simulation using machine learning techniques, the nonlinear characteristics of structures are formulated into a surrogate element to replace the original mechanical elements, then the dynamics simulation is accomplished by co-simulation via embedding the surrogate element into the MB model. This framework consists of a series of techniques including the data collection and feature extraction, the training data sampling, the surrogate element building, and the model evaluation and selection. To verify the accessibility of this framework, two case studies of a vertical and a longitudinal vehicle dynamics simulation are carried out based on Simulink/Simpack co-simulation. By comparing two data-driven models (the Legendre polynomial regression (LPR) and the Kriging), the result shows that using the LPR model in building surrogate elements can largely cut down the simulation time without much compromising of the accuracy.

Keywords: Dynamics simulation; Data-driven modelling; Machine learning; Surrogate element; Co-simulation

1. Introduction

In vehicle dynamics studies, the most reliable approach in investigating the dynamics behaviours of railway vehicles is to take a full-size test of the whole train. In the SAFETRAIN project supported by the European Commission, both dynamic and static tests were carried out in investigating the structural crashworthiness of vehicle ends in order to improve the passive safety [1]. In 2003, to assess the crashworthiness performance of passenger trains, the U.S. Department Of Transportation conducted two full-scale collision tests with the conventional and the CEM (Crash Energy Man-

agement) passenger vehicles crashing with a wall, and analysed the motion details of the passenger cars [2]. In 2006, to improve the occupant safety, a further full-scale train-to-train crash test was carried out on a passenger train equipped with the CEM equipment and the conventional crush zone designs [3, 4].

Due to the high economic cost of full-scale tests, scaled tests are adopted. For instance, the application of scaled roller rigs for railway vehicle bogies has got a widespread development in studying the dynamics since an early age, and now it still shows prospects in designing new devices and technologies [5-7]. Li et al. conducted collision tests using several simplified vehicle models to investigate the energy absorption and dissipation pattern of the honeycomb-based structures in train-to-train crash scenarios [8]. To decrease the wheel-rail wear for vehicle bogies, Kim et al. designed an active steering control system and tested it with a 1/5 scaled vehicle on a curved tract to assess the performance of this system [9]. A scaled test can save cost though, it still demands for enormous human labour and substantial cost to design and make every subtle structures.

With the increasing progress of Computer Aided Engineering, the simulation technology has largely helped to cut down the research expenditure and the labour cost in vehicle dynamics study. Among the traditional vehicle dynamics simulation methods, the finite element (FE) method and the multi-body (MB) method are two powerful simulation tools, where the FE method related techniques mainly focus on investigating the stress and strain details of the whole train or its substructures during a dynamic process. For example, in the occupant safety and protection study, the FE method was usually used in the crashworthiness performance assessment for passenger vehicles [10-13]. It also took up a wide application field in the vehicle collision research and the post-derailment behaviour analysis, especially for the collision leaded derailment investigations [7, 14]. Besides, in the wheel-rail contact research, researchers generally choose FE method to simulate the highly nonlinear dynamic contact in the running stage [15].

Taking the complexity of the whole train into consideration, although using the FE method can build a detailed model for each substructure and reach a high accuracy [16-18], it is inevitable that the FE method demands for a large amount of time, especially for those involved in an iteration and optimisation process for designing train’s

structures. Moreover, when it comes to the highly nonlinear dynamic problems (e.g. large deformation in collision), a rigorous FE analysis relies on good mesh quality and a precise control in hourglass energy [19, 20].

An alternative for the FE method is the MB method. As a simplified simulation tool, it has been widely applied in solving dynamics problems involving multiple vehicles, especially in the train's running performance analysis on different tracks [21-23], the security, stability and comfort assessments for passenger vehicles [24], and the dynamic interaction simulation between vehicles or substructures during the train crash process [25-27]. Because of the simplification, the MB method runs fast, but when coming to representing highly nonlinear patterns in the dynamics, the MB method is still time-consuming and only offers a limited accuracy [28].

To balance an acceptable accuracy and a satisfying efficiency, the data-driven simulation method as a reverse engineering technology has got an increasing attention recently in vehicle engineering. Dias et al. took the test data and the FE simulation results during a collision between end structures as the training data. With these data, the step-wise function was used to fit a force-displacement curve during the deformation period of an end structure, which was applied in the crashworthiness design [29, 30]. Taheri et al. introduced the machine learning techniques to the vehicle dynamics, where MB simulation data were applied to train the Kriging model in building a surrogate element which was used to replace all the force elements in the second suspension system of a vehicle's MB model [31]. In the aspect of the structure crashworthiness design, Forsberg et al. and Xie et al. used the data from FE simulation to train the Kriging model and the polynomial response surfaces, which were used as the surrogate models to avoid iterations with using the FE method. Then optimisation algorithms were applied in the surrogate models to acquire better parameters in structure design such as for energy absorbing tubes [32-34] and inner parts of vehicles [35].

In this paper, a framework for the data-driven simulation was presented. It consists of a series of essential techniques in constructing a surrogate element including the data collection and feature extraction, the training data sampling, the surrogate element building, and the model evaluation and selection. In the end of this paper, two case studies were carried out to assess the performance of this framework. The struc-

ture of this paper is shown as follows: the main process and the methods involved in the framework are explained in section 2; section 3 is the theory part about all the methods used in the data-driven simulation framework; two cases studies conducted for assessing the performance of this framework are presented in section 4, and the evaluation for using the two data-driven models (the Legendre polynomial regression (LPR) and the Kriging) is elaborated in section 4.2, then the summary about the contributions of this paper is put in section 5.

2. Overview

To give an overview of this paper, the structure and the procedures of the data-driven simulation framework are presented in Figure 1 which illustrates the main functions of each technique used in the data-driven simulation. The framework of this simulation process is divided into four parts:

- Data collection and feature extraction

The first task to build a data-driven surrogate element is deciding what kind of dynamics pattern the data-driven model needs to learn. The data which reflects the mechanical characteristics of a structure need to be collected first (e.g. the post-processing data from FE models or test data) and extracted into the training data that our model could learn from to build the surrogate element. A specific feature extraction is designed to fit a particular simulation task, where a further discussion will follow in this paper.

- Training data sampling

In general engineering practices, it is common that there are a large amount of training data from a simulation or a test. Some of these could be redundant, repeated or have a same pattern and high relativity with others, and such redundancy could bring a low computation efficiency or a singularity problem in further computation. To improve the overall performance of our method, a sampling technique is used to filter the training data into the training samples which can largely represent the original data and is processed to build a surrogate element.

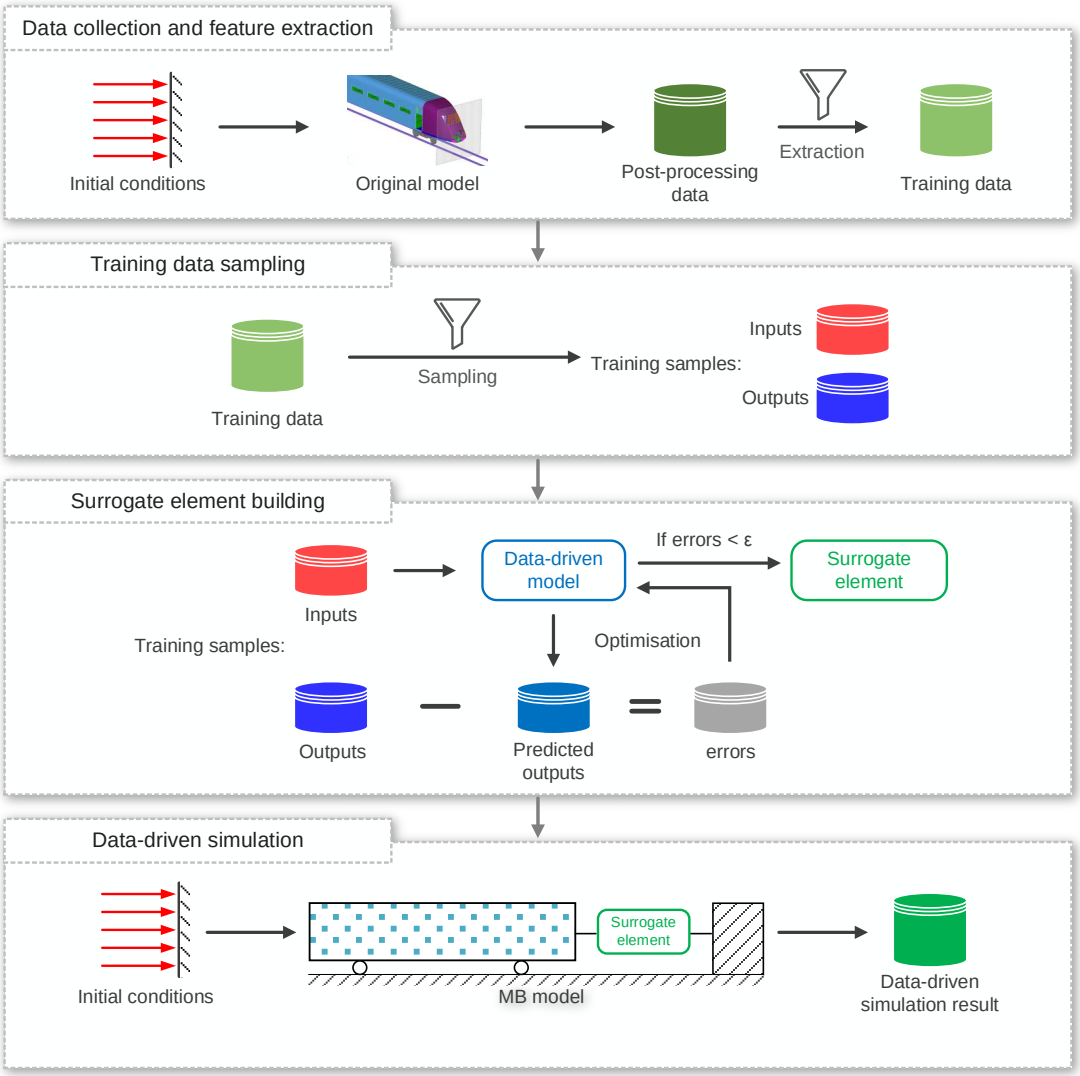

Figure 1. The data-driven dynamics simulation framework

- Surrogate element building

After acquiring the training samples, a data-driven maps the implicit relationship from the inputs to the outputs accordingly. To refine the data-driven model, the parameters in it are iterated by an optimisation algorithm to minimise the mapping errors between the outputs from the training samples and the predicted ones. Once the errors satisfy a threshold, an optimised data-driven model is built and can be used as a surrogate element that represents the dynamics characteristics of some force element(s).

- Data-driven simulation

Using the surrogate element to replace some specific element(s) which acts as the counterpart in the FE model, and keeping the other specifications (e.g. initial condi-

tions, structure parameters and constraints) in the same, then the data-driven simulation is configured.

Each simulation task customaries its specific feature extraction, and in this paper we respectively made a discussion about how to design feasible data-driven models in simulating the vertical dynamics of a vehicle's suspension system in running and the longitudinal dynamics of a train set (with a lead car and a passenger car) in a crash.

3. Methodology for data-driven simulations

The details of the techniques contained in Figure 1 are elaborated in this section, and we divided it into four parts based on the four main procedures in a data-driven simulation.

3.1. Data collection and feature extraction

- Feature extraction for vertical dynamics simulations

For vertical dynamics simulations, we described our model in Figure 2. The primary function of a surrogate element is to replace all the force elements involved in the second suspension system which has highly nonlinear characteristics and is hard to be modelled or time-consuming to be simulated.

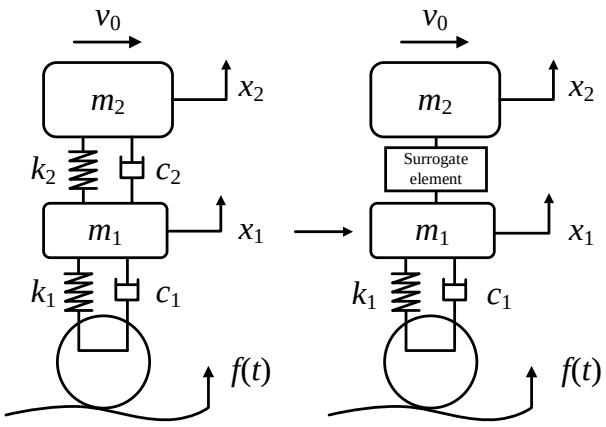

Figure 2. A surrogate element in vertical dynamics simulations

In Figure 2, m_1 and m_2 respectively represent the mass value of the bogie and the body of a vehicle; x_1 and x_2 are the displacements of the bogie and the vehicle body taking the rail as the reference system; k_1, c_1, k_2, c_2 stand for the vertical stiffness coefficients and the vertical damping coefficients of the first and the second suspension systems respectively, where k_2, c_2 are unknown or difficult to determine.

$f(t)$ is the random vibration from the track and v_0 is the running speed of this vehicle. The dynamics equations in Figure 2 can be written as

$$\begin{bmatrix} m_1\ddot{x}_1 \\ m_2\ddot{x}_2 \end{bmatrix} = \begin{bmatrix} f(t) - k_1x_1 - c_1\dot{x}_1 - k_2(x_1 - x_2) - c_2(\dot{x}_1 - \dot{x}_2) \\ k_2(x_1 - x_2) + c_2(\dot{x}_1 - \dot{x}_2) \end{bmatrix}. \tag{1}$$

Since k_2, c_2 are unknown, x_1 and x_2 cannot be solved from the equation system. However, from the formula (1), the acceleration value $\ddot{x}_2$ is decided by the spring force $k_2(x_1 - x_2)$ and the damping force $c_2(\dot{x}_1 - \dot{x}_2)$ which contains the information about k_2 and c_2, and that information is the pattern that our data-driven model needs to learn to build a surrogate element. In this case, we chose $\boldsymbol{u} = (x_1 - x_2, \dot{x}_1 - \dot{x}_2)^{\mathrm{T}}$ as the two-dimensional input and the $v = m_2\ddot{x}_2$ as the output of the training data. Then the goal of the data-driven model is to present the relationship $v = \mathrm{F}(\boldsymbol{u})$ where the information about k_2 and c_2 are expressed implicitly. After that, the dynamics formula containing a surrogate element can be rewritten as

$$\begin{bmatrix} m_1\ddot{x}_1 \\ m_2\ddot{x}_2 \end{bmatrix} = \begin{bmatrix} f(t) - k_1x_1 - c_1\dot{x}_1 - \mathrm{F}(x_1 - x_2, \dot{x}_1 - \dot{x}_2) \\ \mathrm{F}(x_1 - x_2, \dot{x}_1 - \dot{x}_2) \end{bmatrix}. \tag{2}$$

- *Feature extraction for longitudinal dynamics simulations*

As to longitudinal dynamics simulations, the function of the surrogate elements is depicted in Figure 3. Two surrogate elements are embedded in the MB model to replace the energy absorbing structures (or deformable structures, e.g. couplers and end structures) in the FE model.

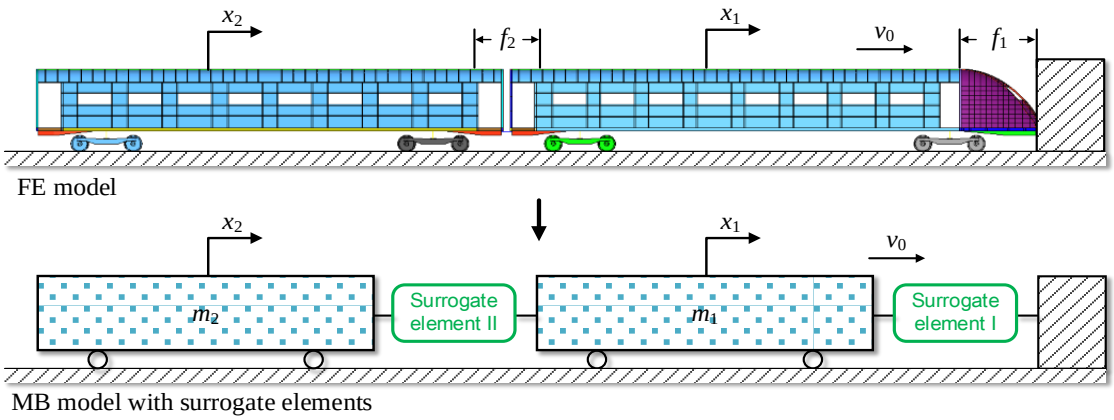

Figure 3. Surrogate elements in longitudinal dynamics simulations

Similar to the vertical dynamics case, the motion equations of the two vehicle bodies are represented as

$$\begin{cases} m_1\ddot{x}_1 = -k_1 x_1 - k_2(x_1 - x_2) - (m_1 \mathrm{g} \cdot f_c) \cdot \mathrm{I}(\dot{x}_1) \\ m_2\ddot{x}_2 = \quad k_2(x_1 - x_2) - (m_2 \mathrm{g} \cdot f_c) \cdot \mathrm{I}(\dot{x}_2) \end{cases}, \tag{3}$$

where m_1, x_1, m_2, x_2 respectively represent the mass value and the longitudinal displacement of the lead car and the passenger car during the crash period. k_1 and k_2 are the equivalent stiffness value of the energy absorbing structures in the lead car and the passenger car. g is the acceleration of gravity and f_c is the friction coefficient between the wheel-rail. $\mathrm{I}(\cdot)$ is the indicator function used to determine the direction of the friction force. Since the curves of k_1 and k_2 are highly nonlinear and consist of the cyclic loading and unloading stages during the crash, it is hard to figure them out. Then we used the data-driven model to extract the information of k_1 and k_2 into functions $f_1 = \mathrm{G}_1(x_1)$ and $f_2 = \mathrm{G}_2(x_1 - x_2)$, where f_1 is the interaction force between the wall and the lead car, and f_2 is the interaction force between the lead car and the passenger car, and there are the relationships $f_1 \approx k_1 x_1$ and $f_2 \approx k_2(x_1 - x_2)$. In this case, four data-driven models are needed to learn the loading stage and the unloading stage of k_1 and k_2 respectively. x_1 and f_1 are chosen as the input and the output of the first training data. $x_1 - x_2$ and f_2 act as the input and the output of the second data. The formula (3) can then be rewritten as

$$\begin{cases} m_1\ddot{x}_1 = -\mathrm{G}_1(x_1) - \mathrm{G}_2(x_1 - x_2) - (m_1 \mathrm{g} \cdot f_c) \cdot \mathrm{I}(\dot{x}_1) \\ m_2\ddot{x}_2 = \quad \mathrm{G}_2(x_1 - x_2) - (m_2 \mathrm{g} \cdot f_c) \cdot \mathrm{I}(\dot{x}_2) \end{cases}. \tag{4}$$

After the feature decisions, the training data can be collected from the post-processing data of a complex simulation model or a test. In the vertical dynamics, the simulation data from a highly nonlinear MB model were used as the data source, and in the longitudinal dynamics, we mainly used the post-processing data from a FE model.

3.2. Training data sampling

Since there could be redundant information among the training data, a data sampling process is recommended. For the reason that a sampling plan has a large effect on the accuracy and efficiency of a data-driven model, the sampling plan developed by Taheri et al. was introduced to pick the training samples in this paper [31]. The idea of this sampling plan is to select the optimal M samples $\boldsymbol{U} = \left(\boldsymbol{u}^{(1)}, \boldsymbol{u}^{(2)}, \ldots, \boldsymbol{u}^{(M)}\right)^{\mathrm{T}}, \boldsymbol{u}^{(*)} \in \boldsymbol{X} \subset \mathbf{R}^{\mathrm{D}}$ from the training data set $\boldsymbol{X}$, such that $\boldsymbol{U}$

can mostly spatially fill the data set $\boldsymbol{X}$, where D is the dimension of $\boldsymbol{u}^{(*)}$.

To test the accessibility of this method, 1600 two-dimensional points were randomly scattered in the space $[0,1] \times [0,1]$, and among them we selected the best 36 samples using the genetic algorithm [36]. The sampling result are shown in Figure 4. Through the sampling process, the training inputs $\boldsymbol{U} = \left(\boldsymbol{u}^{(1)}, \boldsymbol{u}^{(2)}, \dots, \boldsymbol{u}^{(M)}\right)^{\mathrm{T}}$ and their outputs $\boldsymbol{V} = \left(v^{(1)}, v^{(2)}, \dots, v^{(M)}\right)^{\mathrm{T}}$ are prepared to train the data-driven model.

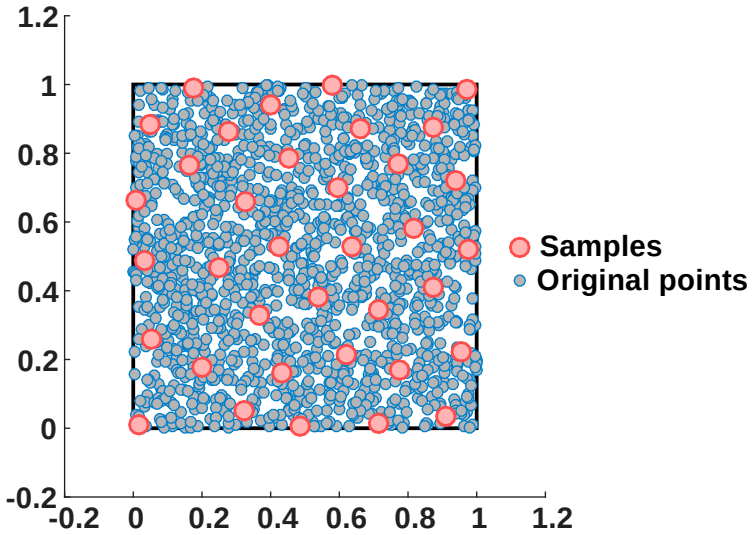

Figure 4. Selecting the best 36 samples from 1600 points

3.3. Surrogate element building

Since the Legendre polynomials are a kind of orthogonal polynomial sequence [37] which ensures a stable and efficient solution in solving the regression parameters even with a high degree [38, 39], in this section we use the Legendre polynomial regression (LPR) model to map the nonlinearity $v = \mathrm{F}(\boldsymbol{u})$ between the input $\boldsymbol{u}$ and the output v of training samples. We denote u_d as the d th dimensional input of $\boldsymbol{u}$ ($d = 1,2, \dots, \mathrm{D}$). The output v is generally one-dimensional. In section 3.1, there are $\mathrm{D} = 2$ in the first case and $\mathrm{D} = 1$ in the second case. In this part, we mainly discuss the regression method with $\mathrm{D} = 2$ case and it is also suitable when $\mathrm{D} = 1$.

Since the relationship $v = \mathrm{F}(\boldsymbol{u})$ is the target the LPR model need to learn (or fit) from the training samples, we construct the LPR model $\hat{\mathrm{F}}(\boldsymbol{u})$ to approximate $\mathrm{F}(\boldsymbol{u})$ as the following expression shows

$$\hat{v} = \hat{\mathrm{F}}(\boldsymbol{u}) = \sum_{i=0}^{n_1} \alpha_i p_i(u_1) + \sum_{j=0}^{n_2} \beta_j p_j(u_2),$$

$$v = \mathrm{F}(\boldsymbol{u}) = \hat{v} + e, \tag{5}$$

where two Legendre polynomial sequences $\{p_i\}$ and $\{p_j\}$ are used, and $\hat{v}$ is the prediction value of v; e is the approximation error; p_i, p_j are the elements of the two sequences; α_i, β_j are the coefficients of these elements, which are determined by training; n_1, n_2 respectively represent the degree of the two polynomial sequences, where $i = 0,1, \ldots n_1, j = 0,1 \ldots n_2$.

In equation (5), we solve the fitting problem using the decoupled two-variable Legendre polynomial regression because the equation in (1) indicates the following relationship

$$m_2\ddot{x}_2 = k_2(x_1 - x_2) + c_2(\dot{x}_1 - \dot{x}_2) \rightarrow v = k_2u_1 + c_2u_2,$$

which theoretically means no cross factor between u_1 and u_2 acting on the output v.

After that, u, v in equation (5) are replaced with training samples $\{\boldsymbol{U}, \boldsymbol{V}\}$ to solve the coefficients $\{\alpha_i, \beta_j\}$ (see equation (6)).

$$\begin{bmatrix} v^{(1)} \\ v^{(2)} \\ \vdots \\ v^{(M)} \end{bmatrix} = \begin{bmatrix} p_0(u_1^{(1)}) & \cdots & p_{n_1}(u_1^{(1)}) & p_0(u_2^{(1)}) & \cdots & p_{n_2}(u_2^{(1)}) \\ p_0(u_1^{(2)}) & \cdots & p_{n_1}(u_1^{(2)}) & p_0(u_2^{(2)}) & \cdots & p_{n_2}(u_2^{(2)}) \\ & & & \vdots & & \\ p_0(u_1^{(M)}) & \cdots & p_{n_1}(u_1^{(M)}) & p_0(u_2^{(M)}) & \cdots & p_{n_2}(u_2^{(M)}) \end{bmatrix} \begin{bmatrix} \alpha_0 \\ \vdots \\ \alpha_{n_1} \\ \beta_0 \\ \vdots \\ \beta_{n_2} \end{bmatrix} + \boldsymbol{e}. \tag{6}$$

Since equation (6) is generally overdetermined, the least square solution of $\{\alpha_i, \beta_j\}$ can be acquired by solving the normal equation

$$\boldsymbol{P}^T\boldsymbol{P}\boldsymbol{\alpha} = \boldsymbol{P}^T\boldsymbol{V}, \tag{7}$$

where $\boldsymbol{P}$ is the coefficient matrix in equation (6) and $\boldsymbol{\alpha}$ is the least square solution of the coefficients $(\alpha_0, \cdots, \alpha_{n_1}, \beta_0, \cdots, \beta_{n_2})^{\mathrm{T}}$ in equation (5).

Finally, the LPR model $\hat{\mathrm{F}}(\boldsymbol{u})$ is constructed to act as a surrogate element in equation (2). As for the second case in section 3.1, two one-variable LPR models are demanded to build the surrogate elements, which is similar to this process.

3.4. Model evaluation and selection

If there are several data-driven models, it is significant to choose proper test samples to compare the performance of these models. In machine learning, the cross validation is an important procedure after building several models, which is a method splitting the training data into training samples and test samples in many different ways, then using the training samples to train these models and the test samples to validate these models, and finally to vote which model or which model parameters are the "best" on average [40]. In this paper, since the degree of the Legendre polynomials needs to be decided first, we use the samples that are filtered out from the training data set $\boldsymbol{X}$ as the test samples **(**known as the OOB (out of bag) samples [41] **)** to decide the polynomial degree.

As for how to define the "best", there are many references for measuring a model's performance from different aspects. We presented four indexes to evaluate the performance of a data-driven model.

- Prediction accuracy

If the outputs of test samples are far from the zero value, we use the average relative error to assess a model's prediction accuracy.

$$\text{error} = \frac{1}{M\prime} \sum_{i=1}^{M\prime} \left| \frac{\hat{v}_{\mathrm{t}}^{(i)} - v_{\mathrm{t}}^{(i)}}{v_{\mathrm{t}}^{(i)}} \right|. \tag{8}$$

Otherwise the average absolute error is applied.

$$\text{error} = \frac{1}{M\prime} \sum_{i=1}^{M\prime} \left| \hat{v}_{\mathrm{t}}^{(i)} - v_{\mathrm{t}}^{(i)} \right|. \tag{9}$$

In above formulas, $\boldsymbol{U}_{\mathrm{t}} = \left(\boldsymbol{u}_{\mathrm{t}}^{(1)}, \boldsymbol{u}_{\mathrm{t}}^{(2)}, \dots, \boldsymbol{u}_{\mathrm{t}}^{(M\prime)} \right)^{\mathrm{T}}$ and $\boldsymbol{V}_t = \left(v_{\mathrm{t}}^{(1)}, v_{\mathrm{t}}^{(2)}, \dots, v_{\mathrm{t}}^{(M\prime)} \right)^{\mathrm{T}}$ are denoted as the inputs and outputs of test samples, and $\hat{v}_{\mathrm{t}}^{(i)} = \hat{\mathrm{F}}\left(\boldsymbol{u}_{\mathrm{t}}^{(i)} \right)$ is the i th predicted output using the data-driven model. M' is the size of test samples.

- Training time and the simulation time

The objects of using the surrogate element is using data to build an accurate vehicle dynamics model. Besides the accuracy, the simulation time is also a key factor. In this part, we denote the simulation time by T_{s}. Since training time is also important in

evaluating the time cost for preparing a data driven model, we denote it by T_t.

- Requirement for the size of training samples

Since in some cases the training data are very rare, under the same accuracy, the model that needs less training samples is the better. Therefore the size of the training samples M is another important index for the performance.

- Tolerance to noises

The training data are generally collected from some specific simulation cases or vehicle tests which are conducted in a specific type of track spectrum. We expect that our data-driven simulation not only has a good performance in that type of track spectrum, but also goes well in different kinds of track spectrum. Hence we collected the training data under one type of track spectrum, and used it to train our model to get the surrogate element then applied it in calculating the simulation cases under different kinds of track spectrum to evaluate our model's tolerance to noises.

4. Case studies

To verify the accessibility of the data-driven dynamics simulation framework, in this section two case studies were carried out. In the first one, the usage of this framework in a common vertical dynamics simulation was elaborated, and a comparison of two data-driven models (the LPR model and the Kriging model [31]) was made to verify the performance of these models; In the second one, we used the LPR model to build the surrogate element and gave a detailed description in the longitudinal dynamics simulation in a train crash. All the simulations in this section were carried out on the platform of Window 7 64bit with two CPUs (Intel Xeon X5680 3.33GHZ) and 32.0 GB RAM.

4.1. Vertical dynamics simulation

As Figure 2 and section 3.1 described, to build a surrogate element for the second suspension system, we collected the training data from the post-processing results of a highly nonlinear MB model built by Simpack. The parameters of the MB model in Figure 2 are detailed in the Table 1, Table 2, Figure 5 and Figure 6.

Table 1. The mass values of the vehicle body and the bogie

Name	m_1	m_2

Value	4600 kg	42000 kg	

Table 2. Parameters of the 5th level of American track spectrum $(f(t))$

Name	A_v	A_a	Ω_s	Ω_c	v_0
Value	0.2095	0.0762	0.8209	0.8245	144 (km/h)

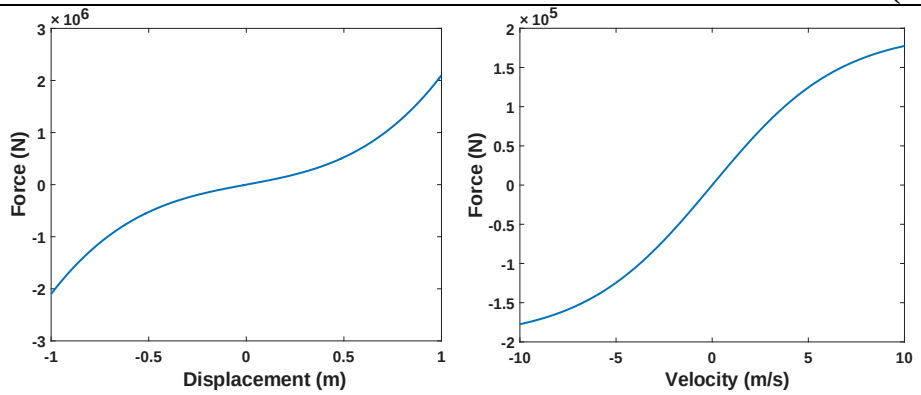

(a) the k_1 curve (b) the c_1 curve

Figure 5. The characteristic curves in the first suspension system

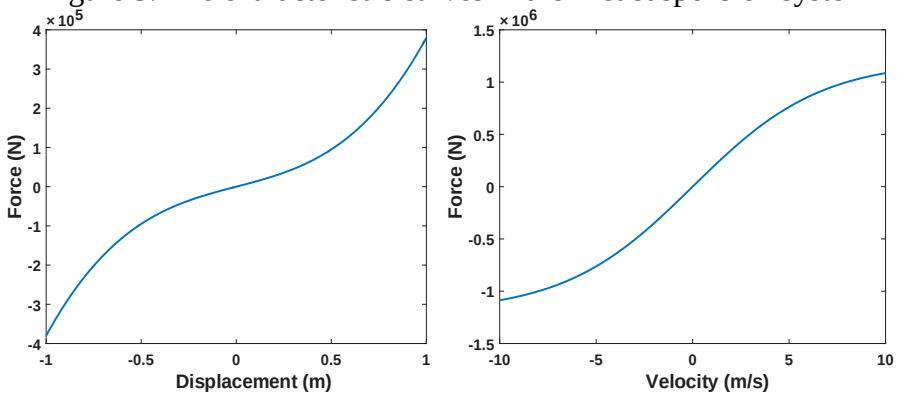

(a) the k_2 curve (b) the c_2 curve

Figure 6. The characteristic curves in the second suspension system

The American track spectrums of four different levels (from 3rd to 6th levels) were used in this section [42]. The parameters shown in Table 2 is at the fifth level which is used to get the training data and build the surrogate element, and the left three levels (3rd, 4th and 6th levels) are used to assess the tolerance ability of data-driven models.

After setting the simulation time at 20 s and sampling rate at 50 Hz in Simpack, the inputs and outputs of training data (1001 points) can be obtained (blue dots in Figure 7). Then applying the data sampling, the training samples (101 points) are acquired (red dots in Figure 7).

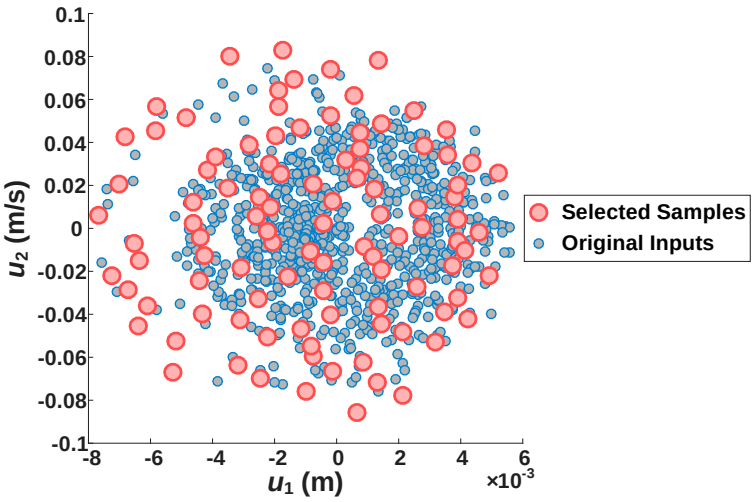

(a) Input samples

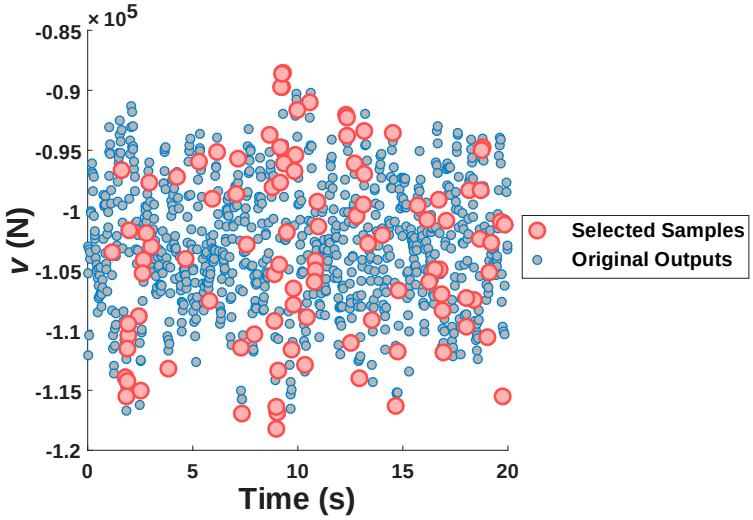

(b) Output samples

Figure 7. Sampling result ($M = 101$)

In Figure 7, the training samples (the selected dots) are used to respectively train the two data-driven models (the LPR model and the Kriging model), and the test samples (the remaining dots) are used to determine the degree of the LPR model and evaluate the performance of the two models. Figure 8 shows the comparison results with using the two trained models to predict the outputs of the test samples.

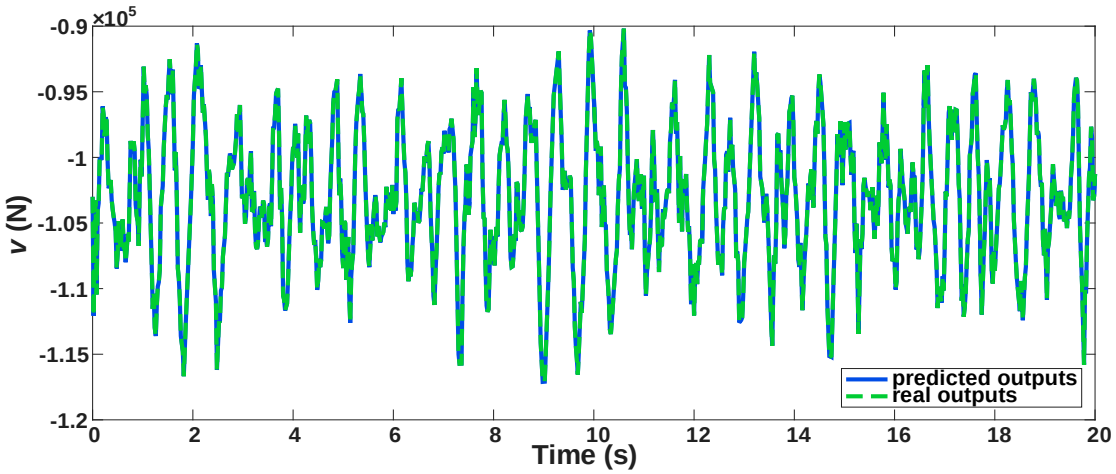

(a) Prediction result using the LPR model $(n_1, n_2 = 3)$

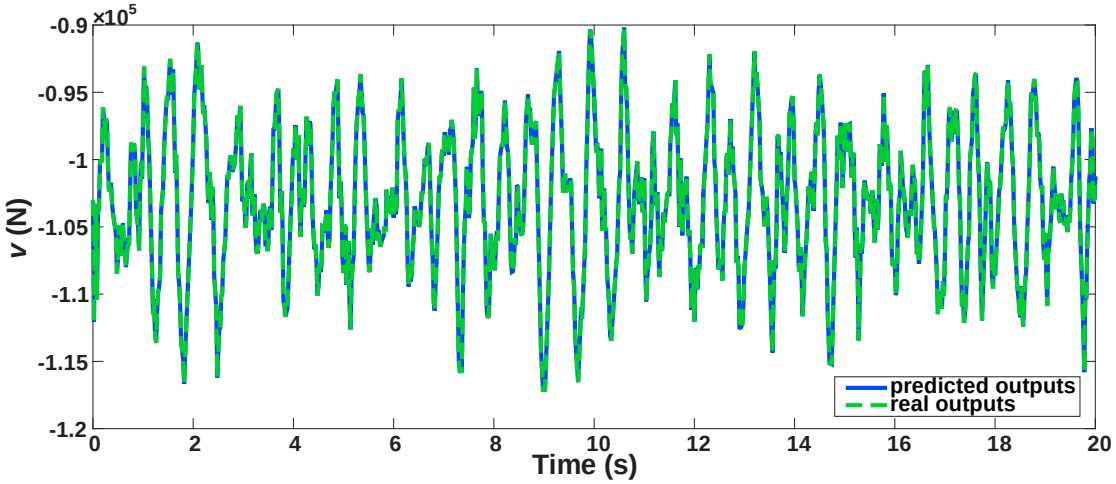

(b) Prediction result using the Kriging model

Figure 8. Predicted outputs of the test samples

Figure 8 shows that the two models both have a great prediction accuracy on test samples. The average relative errors of these two models in prediction are listed in Table 3.

Table 3. The average relative errors of the two models

Model	LPR	Kriging
error	1.92×10^{-8}	1.80×10^{-5}

As the Figure 2 described, we then made the two models acting as the entire second suspension system in the MB model to conduct the data-driven simulation. Based on the Matlab Simulink/ Simpack co-simulation, the calculation result of the vertical acceleration curve of the vehicle body with using the two models are shown in Figure 9, and their average absolute errors are listed in Table 4.

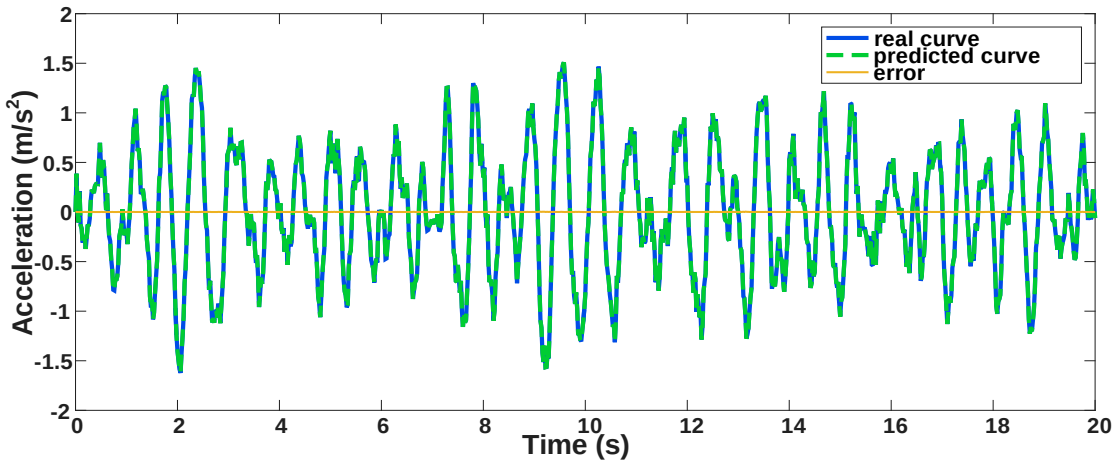

(a) with LPR model

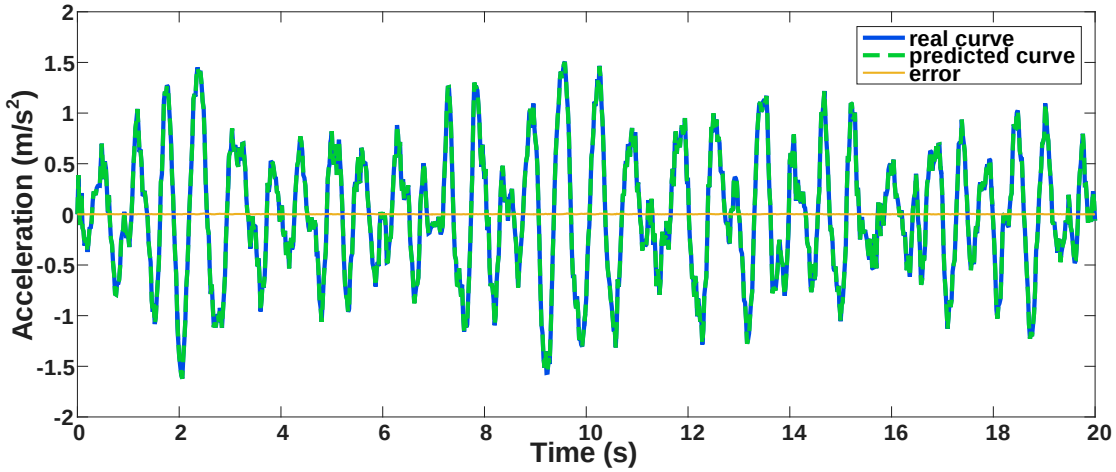

(b) with Kriging model

Figure 9. Acceleration result of data-driven simulations

Table 4. The average absolute errors in acceleration calculation

Model	LPR	Kriging
error	5.67×10^{-4} m/s^2	2.05×10^{-3} m/s^2

The comparison result above shows that the LPR model presents a higher accuracy in the prediction and it can afford a better surrogate element in vertical dynamics simulations. The all-around evaluation of these two models are given in section 4.2.

4.2. Model evaluation for LPR model and Kriging model

Apart from the simulation accuracy, this section mainly focuses on comparing these two models from three aspects: 1. The effect of the size of training samples on a model's simulation accuracy; 2. The time efficiency of training and co-simulation; 3. The tolerance ability for different track spectrums.

- The effect of the size of training samples on models' simulation accuracy

In general, a larger size of training samples can build a stronger data-driven model,

but in some cases the training samples are difficult to access. We should choose the model that has a low demanding for the quantity of samples. Figure 10 displayed another two sampling plans. Then by training the samples with different scales ($M = 51,101,201$), the simulation errors of the vehicle body's displacement, velocity and acceleration curves with using different models are shown in Table 5 and Figure 11.

In Figure 11, the LPR model shows a higher accuracy and it is not sensitive to the size of training samples. It means that the LPR model can maintain a better accuracy with fewer training samples. It also indicates that these samples selected by this kind of sampling method can represent the entire training data very well.

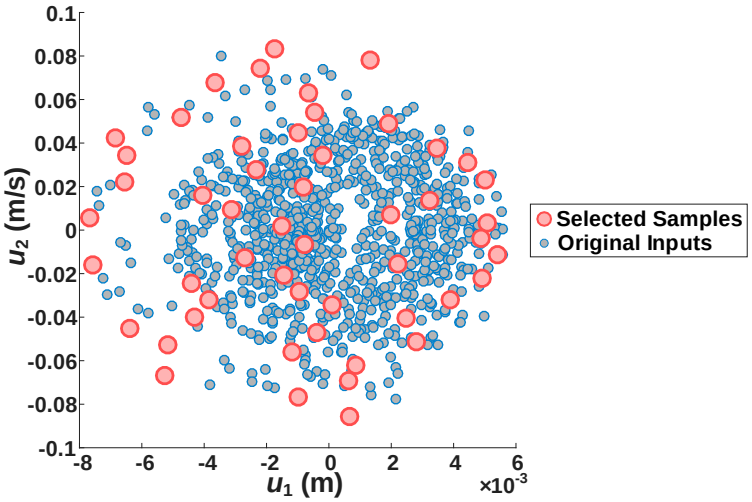

(a) $M = 51$

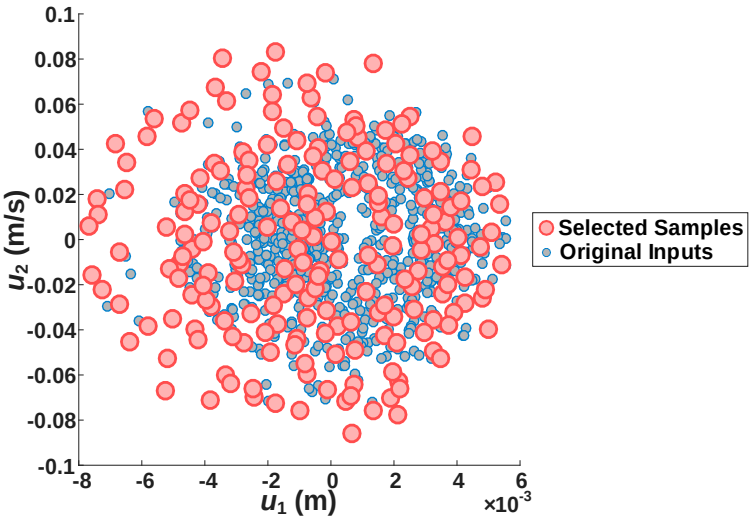

(b) $M = 201$

Figure 10. Different size of selected training samples

Table 5. Simulation errors with using different sampling plans

Model	LPR			Kriging		
Size of samples	51	101	201	51	101	201
Displacement error (m)	2.44E-06	2.44E-06	2.38E-06	1.51E-05	2.10E-05	7.01E-06
Velocity error (m/s)	2.38E-05	2.38E-05	2.38E-05	2.40E-05	1.50E-04	4.64E-05
Acceleration error (m/s^2)	5.67E-04	5.67E-04	5.91E-04	5.70E-04	2.05E-03	8.11E-04

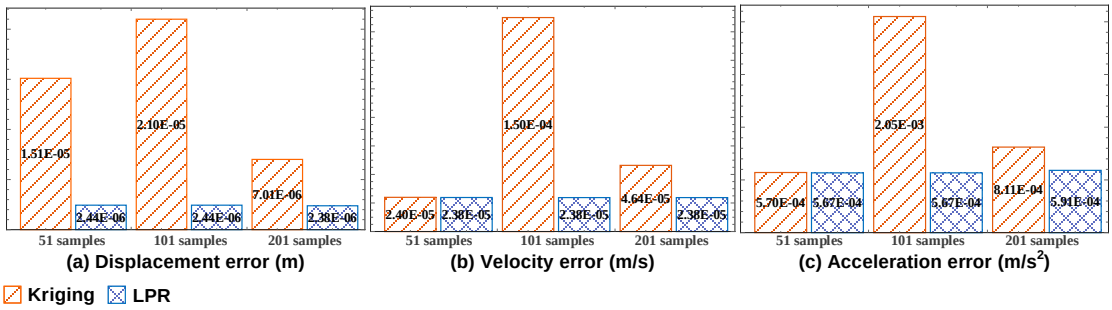

Figure 11. Simulation errors with using different size of training samples

- The time efficiency of training and co-simulation

The time cost for training model, co-simulation and running the original Simpack model are presented in Table 6. It shows that the time cost in training and co-simulation with the LPR model are both low, and it is almost not changed with the increasing size of training samples. Besides that, the time spent in co-simulation is less than that when running the original Simpack model (51.03 s). It means the data-driven model not only keeps a great accuracy, but also save the time, and when it comes to multi-vehicle simulations, this advantage will be more distinct.

Table 6. Time cost of the two models

Model	LPR			Kriging		
Size of samples	51	101	201	51	101	201
Training time $\boldsymbol{T_t}$ (s)	0.08	0.09	0.08	159.27	372.17	1514.09
Co-simulation time $\boldsymbol{T_s}$ (s)	49.64	48.31	50.74	256.35	1593.78	9340.24
Simpack simulation time (s)	51.03					

- The tolerance ability for different track spectrums

In this part, the two models trained in section 4.1 are used to simulate the cases at different levels of track spectrum (see the parameters in Table 7) to test their tolerance ability. The simulation errors of the two models are presented in Table 8.

The results in Table 8 shows that the LPR model have a better accuracy on the whole. For the fourth track's level, the Kriging model diverged, and both the two

models have a lower accuracy than their performance in other cases.

Table 7. Parameters of the 3rd, 4th and 6th levels of American track spectrum [42]

Parameters	Track's level 3rd	4th	6th
$\mathbf{A_v}$	0.6816	0.5376	0.0339
$\mathbf{A_a}$	0.4128	0.3027	0.0339
$\mathbf{\Omega_s}$	0.8520	1.1312	0.4380
$\mathbf{\Omega_c}$	0.8245	0.8245	0.8245
$\boldsymbol{v_0}$ $(\mathbf{km/h})$	96	128	176

Table 8. Simulation errors with different track spectrums

Track's level	LPR			Kriging		
Model	3rd	4th	6th	3rd	4th	6th
Displacement error (m)	4.33E-06	2.70E-03	5.97E-06	4.76E-04	2.95E+02	5.52E-05
Velocity error (m/s)	3.68E-05	2.96E-02	8.57E-05	1.76E-03	5.51E+01	9.42E-05
Acceleration error(m/s^2)	6.70E-04	3.55E-01	4.22E-03	1.78E-02	1.77E+04	2.07E-03

4.3. Longitudinal dynamics simulation

As the Figure 3 and section 3.1 detailed, the training data were collected from the post-processing results of the FE model using LS-DYNA (see Figure 12). The FE model that consists of a lead car and a passenger car is constructed based on our previous work [28, 43]. The parameters involved in the FE model are listed in Table 9.

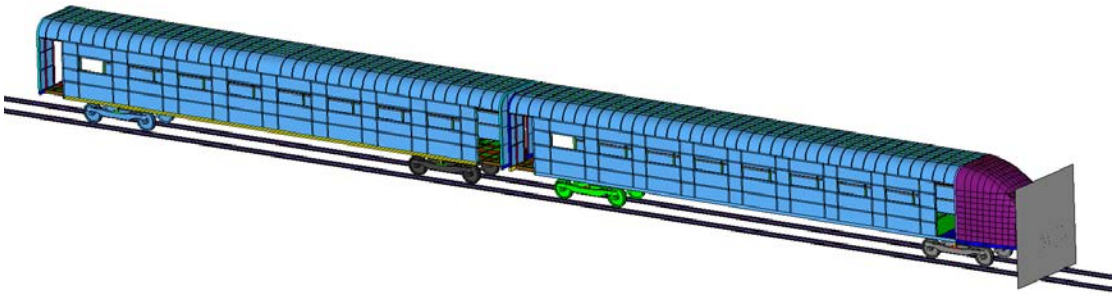

Figure 12. the FE model of two vehicles crashing with a rigid wall

Table 9. Part of the parameters in the FE model

Parameter	Value
Mass of the lead car ($\boldsymbol{m_1}$)	30.39 ton
Mass of the passenger car ($\boldsymbol{m_2}$)	34.45 ton
Length of the lead car ($\boldsymbol{l_1}$)	27.60 m
Length of the passenger car ($\boldsymbol{l_2}$)	24.50 m
Length of the driver's car ($\boldsymbol{l_d}$)	3.93 m
Friction coefficient between wheel-rail ($\boldsymbol{f_c}$)	0.10
Crash velocity ($\boldsymbol{v_0}$)	40 km/h

In Figure 3, since two surrogate elements need to be constructed, we should collect two training sample sets. As the section 3.1 described, the first input-output pair (x_1, f_1) is the lead car's longitudinal displacement and its interaction force with the rigid wall. The second pair $(x_1 - x_2, f_2)$ is the relative displacement between the lead car and the passenger car and their interaction force. Since the inputs of the two training samples both are one-dimensional, the two training sample sets can be illustrated in Figure 13.

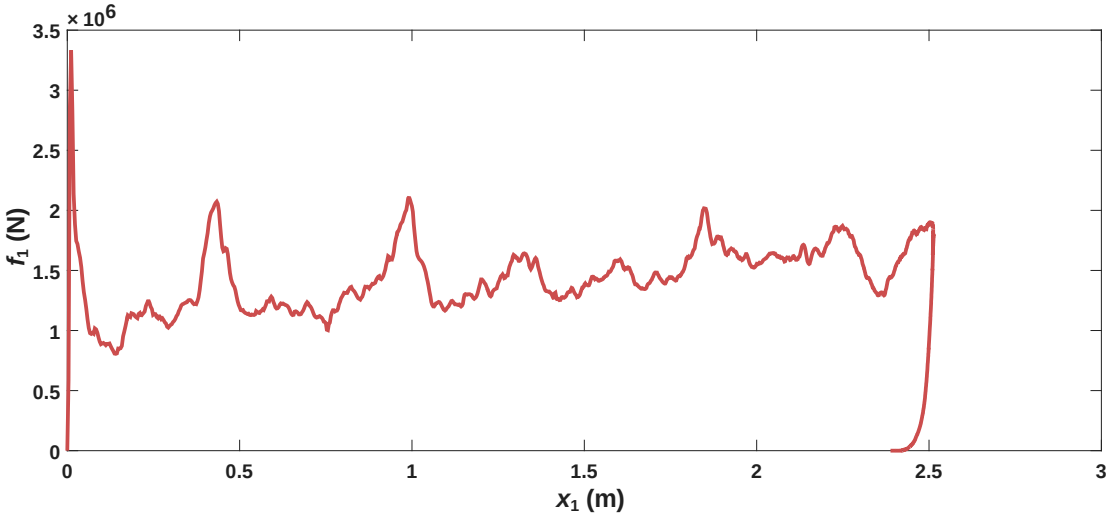

(a) The training samples (x_1, f_1) for the first surrogate element

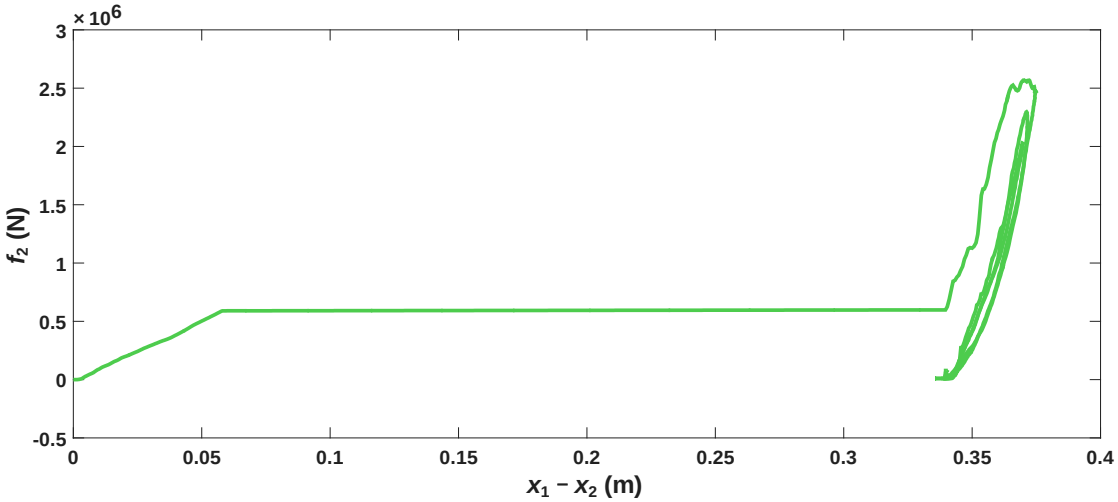

(b) The training samples $(x_1 - x_2, f_2)$ for the second surrogate element

Figure 13. Two training sample sets

Figure 13 shows that the loading and unloading processes cyclically happened between the end structures of the two vehicles during the crash. To build the two surrogate elements for a MB model and make them act as the deformable structures in the FE model, four LPR models are applied to respectively learn the loading and the unloading stages of the relationships $f_1 = \mathrm{G}_1(x_1)$ and $f_2 = \mathrm{G}_2(x_1 - x_2)$. After training the four models, the prediction results on these samples are presented in Figure 14.

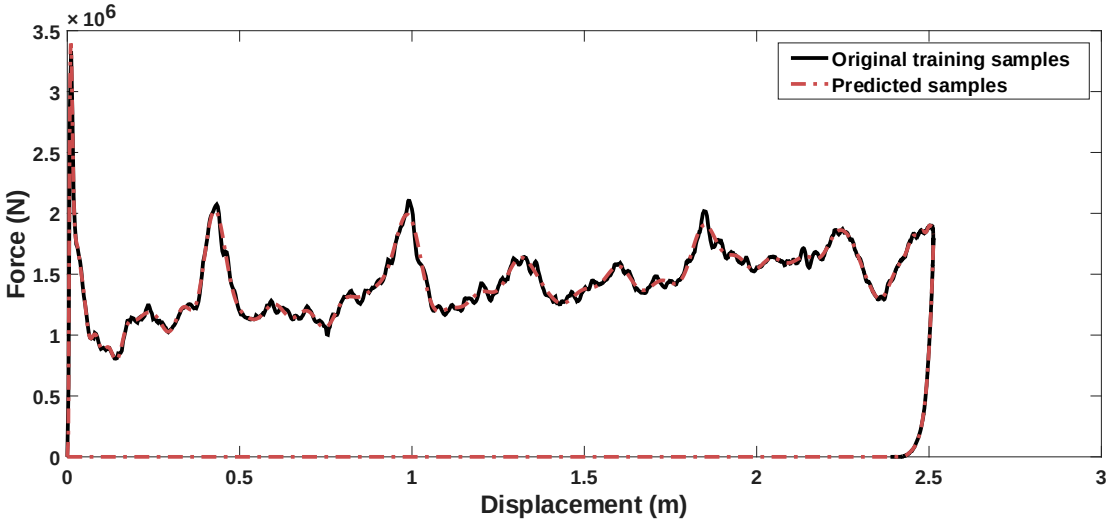

(a) Prediction result of the first training sample set (x_1, f_1)

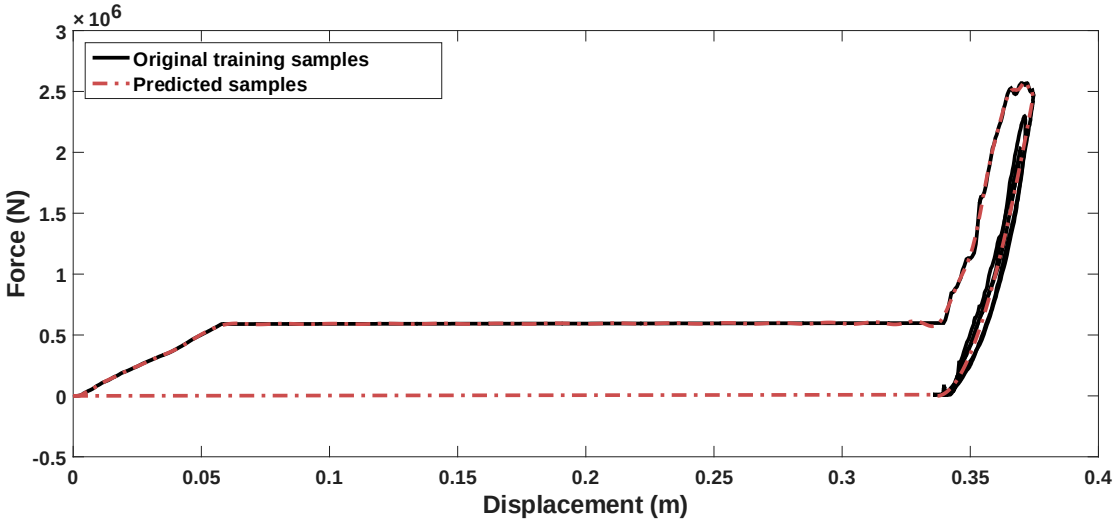

(b) Prediction result of the second training sample set $(x_1 - x_2, f_2)$

Figure 14. Prediction results of the four LPR models

In Figure 14 (a) and (b), we take one LPR model to learn the loading stage and the other one to learn the unloading stage of each vehicle during the entire crash. To choose the best degree for each of the four Legendre polynomials, the ten-fold cross validation method is used and the best degrees are listed in Table 10. By combining these surrogate elements with the MB model in co-simulation, the displacement, velocity and acceleration results of the lead car and the passenger car are obtained, and we compared them with the original data, which are shown in Figure 15.

Table 10. The best degrees for the four Legendre polynomials

Surrogate element	**I**		**II**	
Stage	Loading	Unloading	Loading	Unloading
Degree	69	30	82	5

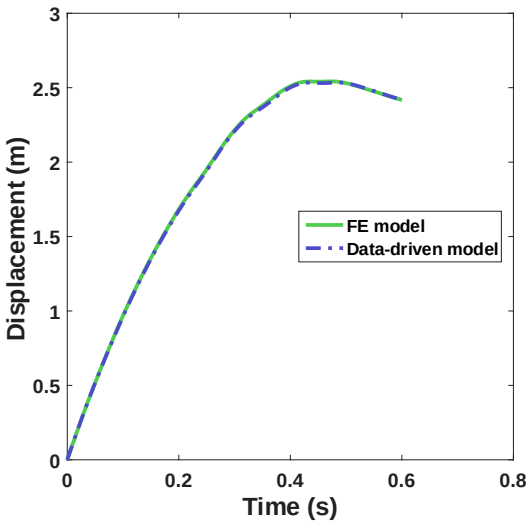

(a) Displacement of the lead car

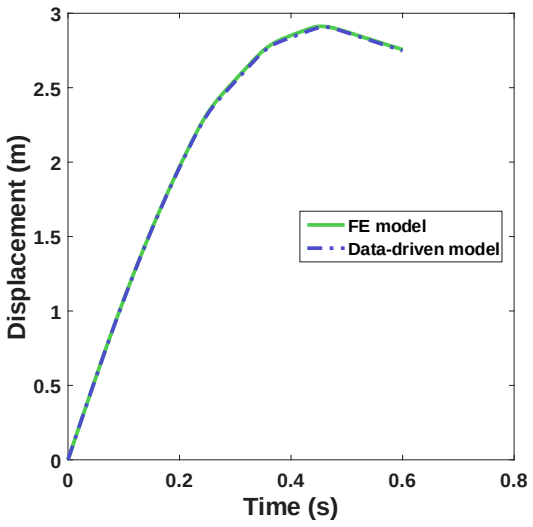

(b) Displacement of the passenger car

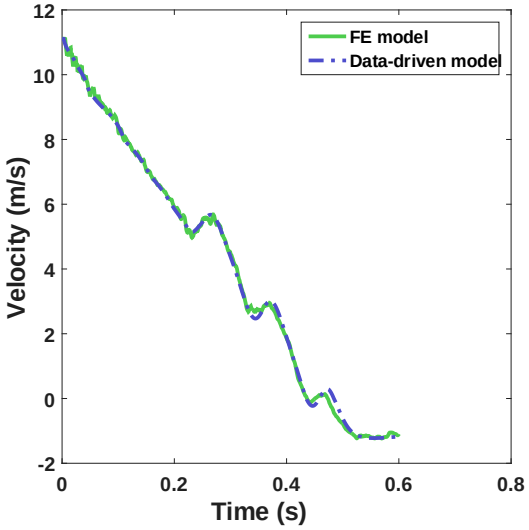

(c) Velocity of the lead car

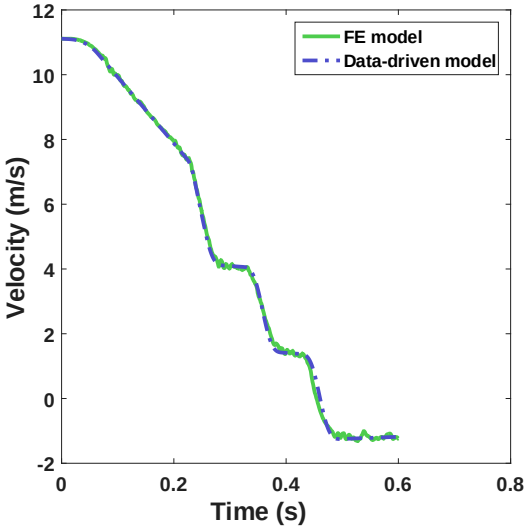

(d) Velocity of the passenger car

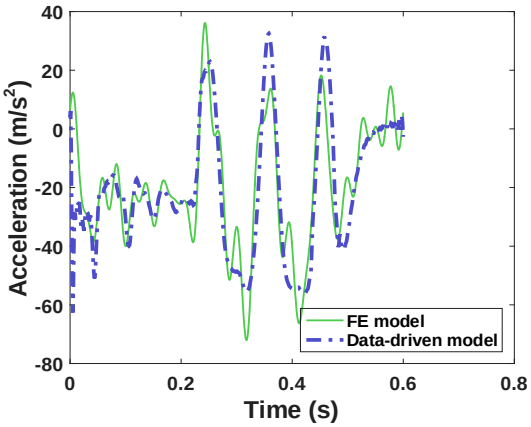

(e) Acceleration of the lead car

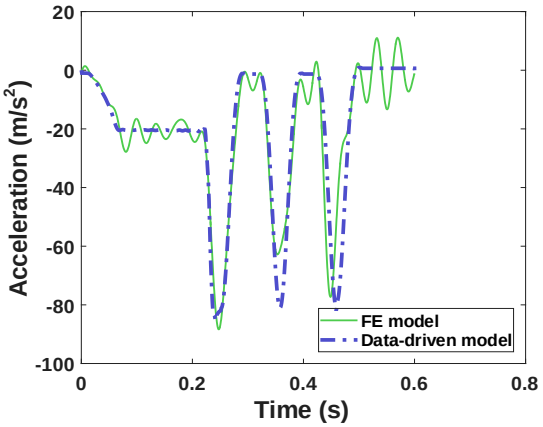

(f) Acceleration of the passenger car

Figure 15. Data-driven simulation results of longitudinal dynamics

The comparison results in Figure 15 indicate that the data-driven simulation converges very well and the overall trends of these curves keep the same with those using FE method, which shows a satisfying accuracy. The time cost of the data-driven co-simulation is about 8 s, while it takes 51548 s when using the FE model. The errors in Figure 15 are detailed in Table 11.

Table 11. The average absolute errors in longitudinal dynamics simulation

	Lead car	Passenger car
Displacement error (m)	0.0063	0.0061
Velocity error (m/s)	0.0957	0.0752
Acceleration error (m/s^2)	8.7122	5.8602

5. Conclusion

To largely reduce the simulation time without at much cost of accuracy, a framework of data-driven simulations for railway dynamics was proposed in this paper. This framework consists of four processes, which use the data from a complex model (a FE model or a real test) to construct surrogate elements to replace those sophisticated structures in the original model. Through embedding these surrogate elements in a MB model, the calculation time can be largely cut down. Two case studies were carried out and it has been proved that both in the vertical and the longitudinal dynamics simulations, the LPR model has a better calculation efficiency with a similar simulation accuracy. By make a comparison with the Kriging model, the main features of the LPR model are shown as follows:

1. The LPR model keeps a high prediction accuracy with using a small size of training samples, and the accuracy is not sensitive to the size of training samples.
2. The time spent in training and co-simulation is short and not sensitive to the size of training samples.
3. The time spent in co-simulation is even less than that with using the original Simpack model, which could be used as a fast calculation approach especially when it comes to multi-vehicle simulations.
4. The Legendre model shows a satisfying stability when simulation cases are involved in different kinds of noises.

From the simulation results of the two case studies, it has been proved that these features made the data-driven models can replace some traditional time-consuming models in further researches.

Acknowledgements

This research was supported and funded by National Natural Science Foundation of China (No. 51405402, No. 51475394); the Independent Research Project of the State Key Laboratory of Traction Power (No. 2015TPL_T06); The Fundamental Research Funds for the Central Universities (No. 2682016CX128) and China Scholarship Council (CSC).

References

[1] M.S. Pereira. Structural crashworthiness of railway vehicles; proceedings of the Proceedings of the 5th World Congress on Railway Research, F, 2006 [C].

[2] K. Jacobsen, D. Tyrell, B. Perlman. Impact Tests of Crash Energy Management Passenger Rail Cars: Analysis and Structural Measurements; proceedings of the ASME 2004 International Mechanical Engineering Congress and Exposition, F, 2004 [C]. American Society of Mechanical Engineers.

[3] D. Tyrell, K. Jacobsen, E. Martinez, et al. Train-to-Train Impact Test of Crash Energy Management Passenger Rail Equipment: Structural Results; proceedings of the ASME 2006 International Mechanical Engineering Congress and Exposition, F, 2006 [C]. American Society of Mechanical Engineers.

[4] K.J. Severson, D.P. Parent. Train-to-Train Impact Test of Crash Energy Management Passenger Rail Equipment: Occupant Experiments; proceedings of the ASME 2006 International Mechanical Engineering Congress and Exposition, F, 2006 [C].

[5] A. Jaschinski, H. Chollet, S. Iwnicki, et al. The Application of Roller Rigs to Railway Vehicle Dynamics [J]. Vehicle System Dynamics, 2010, 31(1999): 345-392.

[6] B. Allotta, L. Pugi, M. Malvezzi, et al. A scaled roller test rig for high-speed vehicles [J]. Vehicle System Dynamics, 2010, 48(S1): 3-18.

[7] H.J. Cho, J.S. Koo. A numerical study of the derailment caused by collision of a rail vehicle using a virtual testing model [J]. Vehicle System Dynamics, 2012, 50(50): 79-108.

[8] R. Li, P. Xu, Y. Peng, et al. Scaled tests and numerical simulations of rail vehicle collisions for various train sets [J]. Proceedings of the Institution of Mechanical Engineers, Part F: Journal of Rail and Rapid Transit, 2016, 230(6): 1590-1600.

[9] M.S. Kim, H.M. Hur, J.H. Park, et al. Performance measurements system of the scaled active steering railway vehicle using the telemetry systems; proceedings of the Wseas International Conference on Signal Processing, Computational Geometry and Artificial Vision, F, 2010 [C].

[10] D. Tyrell, K. Severson, B. Marquis, et al. Locomotive crashworthiness design modifications study; proceedings of the Railroad Conference, 1999 Proceedings of the 1999 ASME/IEEE Joint, F, 1999 [C].

[11] S. Xie, X. Liang, H. Zhou, et al. Crashworthiness optimisation of the front-end structure of the lead car of a high-speed train [J]. Structural and Multidisciplinary Optimization, 2016, 53(2): 339-347.

[12] K.M. Jacobsen. Collision dynamics modeling of crash energy management passenger rail equipment [J]. Dissertations & Theses - Gradworks, 2008, 36(6): 577–580.

[13] A. Scholes, J.H. Lewis. Development of crashworthiness for railway vehicle structures [J]. Proceedings of the Institution of Mechanical Engineers Part F Journal of Rail & Rapid Transit, 1993, 207(16): 1-16.

[14] B. Chen, H. Yang, W. Zhao. Simulation Study of High Speed EMUs Crash [J]. Journal of Dalian Jiaotong University, 2011, 32(1): 11-16.

[15] X. Zhao, Z. Wen, H. Wang, et al. 3D Transient Finite Element Model for High-speed Wheel-rail Rolling Contact and Its Application [J]. Journal of Mechanical Engineering, 2013, 49(18): 1-7.

[16] S. Afazov, W. Denmark, A. Yaghi. Modelling aspects of the design of railway vehicle structures and their crashworthiness [J]. Proceedings of the Institution of Mechanical Engineers, Part F: Journal of Rail and Rapid Transit, 2015, 0954409715605141.

[17] X. Xue, M. Robinson, F. Schmid, et al. Rail vehicle impact analysis: A critique of the suitability of the rigid wall model and the assumption of symmetrical behaviour [J]. Proceedings of the Institution of Mechanical Engineers, Part F: Journal of Rail and Rapid Transit, 2015, 229(2): 173-185.

[18] L. Montalbán, J. Real, T. Real. Mechanical characterization of railway structures based on vertical stiffness analysis and railway substructure stress state [J]. Proceedings of the Institution of Mechanical Engineers, Part F: Journal of Rail and Rapid Transit, 2013, 227(1): 74-85.

[19] H.K. Ibrahim. Design optimization of vehicle structures for crashworthiness improvement [D]; Concordia University Montreal, Quebec, Canada, 2009.

[20] H.-P. Wang, M.E. Botkin, C.-T. Wu, et al. Coupled finite element/meshfree simulation of manufacturing problems; proceedings of the ASME 2003 Pressure Vessels and Piping Conference, F, 2003 [C]. American Society of Mechanical Engineers.

[21] C. Ni, Q. He. Review of Railway Multibody Dynamics Systems [J]. China Academy of Railway Sciences, 1996, 4): 1-11.

[22] H. Cao, W. Zhang, B. Miao. The Vertical Vibration and Suspension Parameters Design of Flexible Car Body for High-speed Railway Vehicles [J]. Mechanical Science and Technology for Aerospace Engineering, 2015, 34(5): 775-779.

[23] J. Zeng, P. Wu. Stability of high speed train [J]. Journal of Traffic and Transportation Engineering, 2005, 5(2): 1-4.

[24] G. Yang, Y. Wei, G. Zhao, et al. Current research progress in the mechanics of

high speed rails [J]. Advances in Mechanics, 2015, 45(201507.

[25] J. Sun, L. Ren, W. Wang. 3D dynamics model and simulation of train crash based on Adams [J]. Computer Aided Engineering, 2013, 22(4): 51-56.

[26] B. Miao, S. Xiao, D. Jin. Research on Modeling and Analysis of a Complex Multibody System by Using Simpack [J]. Mechanical Science and Technology, 2006, 25(7): 813-816.

[27] G. Shen, J. Zhou, L. Ren. Study on Modeling Method for Train Dynamics [J]. Journal of Tongji University (Natural Science), 2004, 24(11): 1-5.

[28] Z. Tang, F.J. Liu, S.H. Guo, et al. Evaluation of coupled finite element/meshfree method for a robust full-scale crashworthiness simulation of railway vehicles [J].

Advances in Mechanical Engineering, 2016, 8(4): 1687814016642954.

[29] J. Dias, M. Pereira. Optimization methods for crashworthiness design using multibody models [J]. Computers & structures, 2004, 82(17): 1371-1380.

[30] J.P. Dias, M.S. Pereira. Analysis and design for train crashworthiness using multibody models [J]. Vehicle System Dynamics, 2004, 40(107-120.

[31] M. Taheri, M. Ahmadian. Machine learning from computer simulations with applications in rail vehicle dynamics [J]. Vehicle System Dynamics, 2016, 54(5): 653-666.

[32] J. Forsberg, L. Nilsson. On polynomial response surfaces and Kriging for use in structural optimization of crashworthiness [J]. Structural & Multidisciplinary Optimization, 2005, 29(3): 232-243.

[33] J. Forsberg, L. Nilsson. Evaluation of response surface methodologies used in crashworthiness optimization [J]. International Journal of Impact Engineering, 2006, 32(5): 759-777.

[34] S. Xie, H. Tian. Optimization Research on the Energy Absorbing Bearing Structure of Railway Vehicle [J]. China Railway Science, 2012, 6): 60-68.

[35] S. Xie, H. Zhou. Optimization on passenger compartment structure of railway vehicle based on Kriging method [J]. Journal of Central South University (Science and Technology), 2012, 43(5): 1190-1198.

[36] A. Chipperfield, P. Fleming. The MATLAB genetic algorithm toolbox [J]. 1995,

[37] J. Dougall. The Product of Two Legendre Polynomials [J]. Proceedings of the Glasgow Mathematical Association, 1953, 1(3): 181-182.

[38] S.C. Narula. Orthogonal polynomial regression [J]. International Statistical Review, 1979, 47(1): 31-36.

[39] J.W. Bright, G.S. Dawkins. Communication. Some Aspects of Curve Fitting Using Orthogonal Polynomials [J]. Industrial & Engineering Chemistry Fundamentals, 1965, 4(1):

[40] C.M. Bishop. Pattern Recognition and Machine Learning (Information Science and Statistics) [M]. Springer-Verlag New York, Inc., 2006.

[41] G. Louppe. Understanding Random Forests [D]; University of Liège, 2014.

[42] V. Garg. Dynamics of railway vehicle systems [M]. Elsevier, 1984.

[43] Z. Tang, Y. Zhu, Y. Nie, et al. Data-driven train set crash dynamics simulation [J]. Vehicle System Dynamics, 2017, 55(2): 149-167.